


Research Article

Active Lane-Changing Control of Intelligent Vehicle on Curved Section of Expressway

Pengfei Feng,^{1,2} Huiqing Jin ,^{1,2} Linfeng Zhao,³ and Mingyu Lu^{1,2}

¹Key Laboratory of Traffic Information and Safety of Anhui Provincial Higher University, Hefei 230601, China

²Anhui Sanlian University, Hefei 230601, China

³School of Automotive and Transportation Engineering, Hefei University of Technology, Hefei 230009, China

Correspondence should be addressed to Huiqing Jin; huiqingjinhfsl@163.com

Received 6 December 2021; Revised 22 March 2022; Accepted 29 April 2022; Published 27 May 2022

Academic Editor: Fahad Al Basir

Copyright © 2022 Pengfei Feng et al. This is an open access article distributed under the Creative Commons Attribution License, which permits unrestricted use, distribution, and reproduction in any medium, provided the original work is properly cited.

In order to improve the intelligent vehicle lane-changing performance, an active lane-changing control algorithm is proposed considering the changes of road curvature and vehicle speed. Firstly, the vehicle dynamics model considering vehicle speed variation and lane-changing safety distance is established, and the expected lane-changing trajectory model under the curved road is designed simultaneously. Then, taking the yaw rate and longitudinal speed as the control objectives of lateral and longitudinal motions, respectively, the sliding-mode variable structure control method based on Lyapunov stability condition is adopted, and the trajectory tracking controller is designed by combining the inverted method to track the desired lane-changing trajectory. Finally, the lane-changing trajectory model and trajectory tracking controller are verified in simulation platform of CarSim/Simulink and hardware-in-the-loop (HIL) test bench. The results show that the proposed trajectory tracking control method can perform the lane-changing behavior well under different road curvatures and vehicle speeds while maintaining high trajectory tracking control accuracy.

1. Introduction

Intelligent vehicle sensors fusion algorithm and intelligent control have become the research hotspots in the field of automotive engineering [1, 2]. As a key technology of intelligent vehicle, active lane-changing can efficiently improve traffic safety, which has attracted researchers' extensive attention [3].

At present, the study of active lane-changing control of intelligent vehicle focuses on lane-changing trajectory planning and tracking control. For the lane-changing trajectory planning, the commonly used trajectory planning methods are utilizing the Bezier curve, spline curve, and polynomial curve. The Bezier curve can solve the desired trajectory according to the selected multiple control points, but the generated trajectory is easily affected by the order and number of control points, which will lead to the discontinuity of the curve [4]. The spline curve can be used to plan the arc trajectory and the sine trajectory, which overcomes the problem of curvature mutation, but the spline curve is

mainly used for static planning [5]. The polynomial curve has been widely used in trajectory planning because of its fast calculation speed, continuous curvature, and real-time control [6–8]. In addition, the reverse trapezoid acceleration curve is used to calculate the desired yaw angle and yaw rate during lane-changing, so as to generate the lane-changing trajectory [9]. Although the trapezoidal acceleration method can be used to design lane-changing trajectory with minimum lateral acceleration, the method is mainly used under straight road conditions [10].

At present, the study of active lane-changing control mainly focuses on straight road. Wang and Wang proposed a lateral switching control strategy based on the dynamics model of the road error [11]. The lateral switching steering controller designed by the strategy improved the path tracking accuracy and stability of the control system. Brown et al. [12] proposed a control framework which combined local path planning and tracking by using the model prediction control (MPC) to realize the vehicle safety and minimum deviation from the target path. Liu

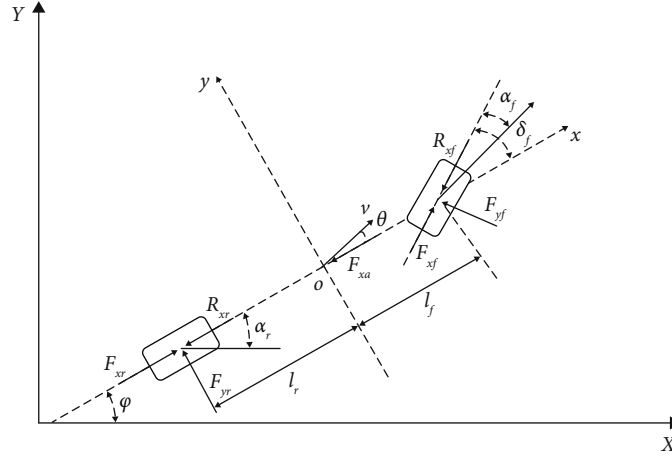


FIGURE 1: The 3-DOF vehicle model.

et al. proposed the preview PID trajectory tracking control by introducing the lane-changing risk coefficient to determine the lane-changing opportunity and realized the lane-changing trajectory tracking control on the straight road [13]. Wang et al. proposed a path tracking algorithm based on the finite element method and steady-state prediction dynamic correction theory [14]. For the curved road conditions, the change of road curvature had a certain impact on the trajectory tracking effect. Peng et al. established an emergency obstacle avoidance safety lane-changing model considering the interaction of “man-vehicle-road” but did not consider the influence of vehicle speed changing [15].

Most of the above algorithms fail to consider the influence of road curvature in lane-changing process and usually set the vehicle speed as a constant value. However, the changing road curvature and vehicle speed are two important influencing factors in lane-changing process; it is necessary to consider their influence in the design of control algorithm. Therefore, the tracking control method of backstepping sliding mode controller is adopted to control the longitudinal and lateral motion of lane changing process in this paper, so as to improve the robustness of intelligent vehicle active lane changing to the change of road environment. Firstly, the vehicle dynamics model is established, and the minimum safe lane-changing distance is established. Then, according to vehicle state constraints at the lane-changing initial and final time, the longitudinal and horizontal lane-changing trajectory planning is carried out under the curved road condition. After that, the steady-state feed-forward control is established, and the backstepping sliding mode trajectory tracking feedback controller is designed to track the lateral trajectory and longitudinal speed. Finally, in order to verify the effectiveness of the proposed control strategy and algorithm, the simulations and hardware-in-the-loop test are carried out under different curve lane-changing conditions. And the results show that by the proposed method good performance in tracking accuracy, lateral motion stability, and robustness to variable road curvature have been obtained.

2. Vehicle Dynamics Model

In order to reduce the calculation parameters and reduce the computational complexity, the vehicle roll and pitch motions are ignored, and the influence of wind speed is not considered. It is assumed that the level of road surface is good and enough tire adhesion can be provided during lane-changing. When the vehicle runs at high speed, the change range of steering wheel angle is in the linear area of tire. Then, the vehicle dynamics model can adopt a vehicle three-degree-of-freedom model with longitudinal and lateral coupling to reflect the longitudinal and lateral motion state changes during the process of vehicle lane-changing [16].

As shown in Figure 1, the state equation of the model can be expressed as

$$\begin{cases} m\dot{v}_x = mv_y\dot{\varphi} + F_{xf} \cos \delta_f + F_{xr} - F_{yf} \sin \delta_f - R_{xr} - R_{xf} \cos \delta_f, \\ m\dot{v}_y = -mv_x\dot{\varphi} + F_{xf} \sin \delta_f + F_{yf} \cos \delta_f + F_{yr} - R_{xf} \sin \delta_f, \\ I_z\ddot{\varphi} = l_f F_{xf} \sin \delta_f + l_f F_{yf} \cos \delta_f - l_r F_{yr} - l_f R_{xf} \sin \delta_f. \end{cases} \quad (1)$$

Since the front-wheel angle of the vehicle is generally small at high speed, it can be approximately considered $\sin \delta_f \approx \delta_f$, $\cos \delta_f \approx 1$. Therefore, the above model be further simplified as

$$\begin{cases} \dot{v}_x = -f_R g + v_y\dot{\varphi} - 2k_1 \frac{v_y + l_f\dot{\varphi}}{mv_x} + \frac{F_x}{m}, \\ \dot{v}_y = \frac{2k_1 + 2k_2}{mv_x} v_y - \left[v_x - \frac{2l_f k_1 - 2l_r k_2}{mv_x} \right] \dot{\varphi} + \frac{\lambda F_x - 2k_1}{m} \delta_f, \\ \ddot{\varphi} = \frac{2l_r k_2^2 + 2l_f k_1^2}{I_z v_x} \dot{\varphi} + \frac{2l_f k_1 - 2l_r k_2}{I_z v_x} v_y + \frac{\lambda F_x l_f - 2l_f k_1}{I_z} \delta_f, \end{cases} \quad (2)$$

where F_{xf} and F_{yf} are the longitudinal and lateral forces on the front wheels, respectively; F_{xr} and F_{yr} are the

longitudinal and lateral forces on the rear wheels, respectively; R_{xf} and R_{xr} are the resistance of the ground to the front and rear wheels, respectively; v_x and v_y are the longitudinal and lateral speeds, respectively; k_1 and k_2 are the cornering stiffness of the front and rear wheels, respectively; $\dot{\varphi}$ represents yaw rate; m is vehicle mass; l_f and l_r are the distance from the center of gravity to the front and rear axles, respectively; δ_f , f_R , c_x , c_z , and θ are used to represent the front steering angle, rolling resistance coefficient, air drag coefficient, air lift coefficient and sideslip angle, respectively; and $\lambda = l_r/(l_f + l_r)$.

3. Lane-Changing Safety Distance Model

When there is an obstacle in front of the vehicle, the vehicle needs to change its lane, and the relative distance between the vehicle and the obstacle can be collected by the sensing module, so as to establish the lane-changing safety distance model and judge whether the distance at the current moment meets the lane-changing requirements in real time.

According to the relative driving state of the front vehicle and the self-vehicle detected by the vehicular sensors, in order to avoid collision, the relative distance between the self-vehicle and the front-vehicle before lane-changing should meet the following condition:

$$d(t) = d(0) + \int_0^t \int_0^\tau (\Delta a) d\tau dt + (\Delta v)t - L - W \sin \theta \geq 0, \quad (3)$$

where $d(0)$ is the distance between the two vehicles at the initial time; Δa and Δv are the relative acceleration and relative speed, respectively; L , W , and θ are the length of the vehicle, the width of the vehicle, and the angle between vehicle speed direction and lane tangent line, respectively.

Therefore, the minimum safety distance between the two vehicles at the initial lane-changing time is

$$d(0)_{\min} = \int_0^t \int_0^\tau (-\Delta a) d\tau dt + (-\Delta v)t + L + W \sin \theta. \quad (4)$$

If the road is curved, the relative distance between the two vehicles obtained from the above formula is the arc distance along the lane line. However, the detection distance of vehicular sensor is the linear distance between two vehicles, so it is necessary to convert the arc distance shown in (4) into the chord distance.

$$l(0)_{\min} = 2R \sin \left(\frac{d(0)_{\min}}{(2R)} \right), \quad (5)$$

where R is the radius of the road centerline.

4. Expected Lane-Changing Trajectory Design under the Curved Road

Safe and reasonable lane-changing tracking is the precondition to achieve the purpose of driving when the vehicle changes its lane or overtakes other vehicles on the curved

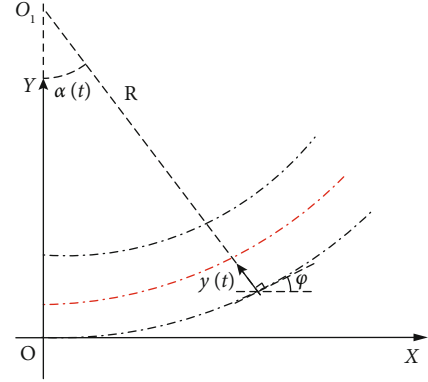


FIGURE 2: Schematic diagram of lane-changing tracking planning.

road. The curvature of the trajectory should be stable and continuous, and the constraints of vehicle dynamics should be satisfied. In this paper, the influence of the remaining vehicles in the target lane in the lane-changing process is not considered when designing the lane-changing tracking on the curved road. It is assumed that the curvature centers o_1 of the inner and outer road centerlines coincide and remain unchanged, and the radius R of the current road centerline is known. The inertial coordinate system is established by taking the vehicle mass centroid at the beginning of lane-changing as the origin. The x -axis is the forward direction along the speed, and the y -axis is perpendicular to the vehicle direction and pointing to the left. The vehicle lane-changing process on the curve road can be divided into the linear motion pointing to the center of the circle and the rotating motion around the circle. The displacement of the linear motion is $y(t)$ and the rotation angle displacement of the vehicle around the o_1 is $\alpha(t)$, shown in Figure 2.

In order to ensure that the lane-changing trajectory meets the characteristics of continuity, smoothness, and monotony, the motion trajectory of linear motion adopts the quintic polynomial. Equation (6) is the general mathematical expression of quintic polynomial function.

$$y(t) = a_{y0} + a_{y1}t + a_{y2}t^2 + a_{y3}t^3 + a_{y4}t^4 + a_{y5}t^5, \quad (6)$$

where t is the lane-changing time, a_{yi} ($i=0, 1, \dots, 5$) is the polynomial coefficient, and $y(t)$ is the lateral displacement.

According to the vehicle motion state before and after lane-changing, the motion conditions of linear motion at the initial time and at the end of lane-changing are as follows:

$$\begin{cases} y(0) = 0, \\ \dot{y}(0) = 0, \\ \ddot{y}(0) = 0, \\ y(t_e) = y_e, \\ \dot{y}(t_e) = 0, \\ \ddot{y}(t_e) = 0, \end{cases} \quad (7)$$

TABLE 1: The simulation parameters.

Name	Value
Vehicle mass m (kg)	1150
Wheelbase L (mm)	2600
Front wheel wheelbase l_f (mm)	1040
Rear wheel wheelbase l_r (mm)	1560
Moment of inertia ($\text{kg} \cdot \text{m}^2$)	1534
Front wheel lateral stiffness k_1 ($\text{N} \cdot \text{rad}^{-1}$)	-65707.9
Front wheel lateral stiffness k_2 ($\text{N} \cdot \text{rad}^{-1}$)	-72489.08
Rolling resistance coefficient f_R	0.02
Air drag coefficient c_x	0.3
Air lift coefficient c_z	0.005

where y_e is the lane width and t_e is the final time of lane-changing. Substituting the constraint conditions in (7) into (6), the trajectory of linear motion is

$$y(t) = \frac{y_e}{t_e^5} (10t_e^2 t^3 - 15t_e t^4 + 6t^5). \quad (8)$$

By calculating the second derivative of equation (8), the a_{re} is

$$a_{re} = \frac{60y_e}{t_e^5} (t_e^2 t - 3t_e t^2 + 2t^3). \quad (9)$$

The longitudinal displacement of the vehicle mass-centroid along the road centerline is changed with sinusoidal acceleration, and the vehicle longitudinal acceleration is designed with sine function.

$$a_x = A \sin \omega t, \quad (10)$$

where A and ω are the amplitude of sine function and angular velocity, respectively.

According to the characteristics of lane-changing behavior, the initial state and final state of the rotation motion around o_1 are as follows:

$$\begin{cases} l_x(0) = 0, \\ \dot{l}_x(0) = v_0, \\ \ddot{l}_x(0) = 0, \\ \dot{l}_x(t_e) = v_e, \\ \ddot{l}_x(t_e) = 0, \end{cases} \quad (11)$$

where v_0 and v_e are the longitudinal speed at the beginning and end of lane-changing, respectively. We make the period of the longitudinal acceleration function be $T = 2t_e$. According to the formula of longitudinal acceleration and the constraint conditions of longitudinal motion, the following equation is obtained:

$$\begin{cases} \int_0^{t_e} A \sin(\omega t) dt = v_e - v_0, \\ \frac{2\pi}{\omega} = T. \end{cases} \quad (12)$$

Then, the coefficients A and ω are computed as

$$\begin{cases} A = \frac{(v_e - v_0)\pi}{2t_e}, \\ \omega = \frac{\pi}{t_e}. \end{cases} \quad (13)$$

By quadratic integration of (10), the trajectory along the road centerline when the vehicle rotates around $l_x(t)$ is obtained.

$$l_x(t) = v_0 t - \frac{A}{\omega^2} \sin \omega t + \frac{A}{\omega} t. \quad (14)$$

The rotational angular displacement $\alpha(t)$ of the vehicle around the center of curvature o_1 is

$$\alpha(t) = \frac{l(t)}{R - y(t)}. \quad (15)$$

The lateral acceleration of the vehicle during lane-changing can be expressed as

$$a_y = a_{re} + \frac{v_x^2(t)}{R} = a_{re} + \frac{[v_0 - (A/\omega)(\cos \omega t - 1)]^2}{R - y(t)}. \quad (16)$$

According to the geometric relationship of vehicle motion, the expected lane-changing trajectory in the inertial coordinate system is related to the road curvature R . Thus, the $X_c(t)$ and $Y_c(t)$ are

$$\begin{cases} X_c(t) = [R - y(t)] \sin \alpha(t), \\ Y_c(t) = R - [R - y(t)] \cos \alpha(t). \end{cases} \quad (17)$$

The desired yaw angle can be expressed as

$$\varphi_d = \arctan \left(\frac{\dot{Y}_c}{\dot{X}_c} \right), \quad (18)$$

where $X_c(t)$ is the longitudinal position of vehicle centroid and $Y_c(t)$ is the lateral position of vehicle centroid.

The transformation relationship between vehicle coordinate system and inertial coordinate system is

$$\begin{cases} \dot{X} = v_x \cos \varphi - v_y \sin \varphi, \\ \dot{Y} = v_x \sin \varphi + v_y \cos \varphi. \end{cases} \quad (19)$$

Under the high-speed driving condition, considering the vehicle stability and riding comfort in the process of lane-changing on the curve road, the longitudinal and lateral

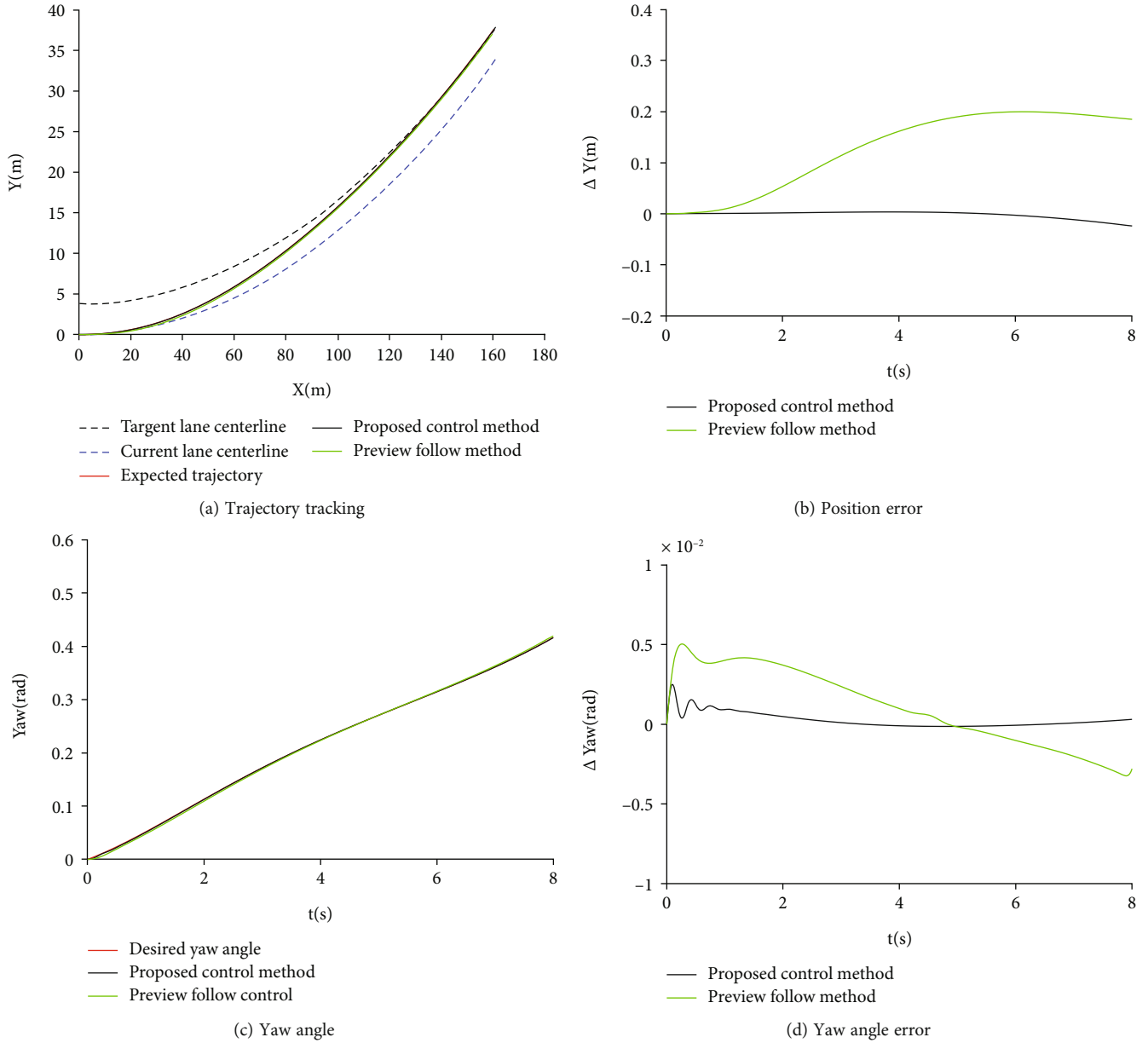


FIGURE 3: Comparison of trajectory tracking control effects.

acceleration needs to be limited within a certain safety range [17], that is,

$$\begin{cases} |a_x| \leq 2 \text{ m/s}^2, \\ |a_y| \leq \min \{0.4g, 0.67 \mu g\}, \end{cases} \quad (20)$$

where g is the acceleration of gravity.

To sum up, considering the road curvature and vehicle state parameters, the lane-changing trajectory in inertial coordinate system shown in (17) can be obtained, and the trajectory meets the vehicle dynamics constraints expressed in (20).

5. Trajectory Tracking Controller Design

In order to track the desired lane-changing trajectory stably, the longitudinal motion control and lateral motion control are needed when the vehicle is changing lanes actively. In this paper, a backstepping sliding mode trajectory tracking controller is designed based on inverted method [18] and sliding mode control theory to realize real-time feedback control of longitudinal and transverse motion of vehicle.

5.1. Lateral Control in Trajectory Tracking. In this paper, the problem of vehicle trajectory tracking control is studied. In the stable lane-changing process, the sideslip angle is very small. Therefore, in order to facilitate the study, only the yaw angle and yaw rate are used as the lateral motion control

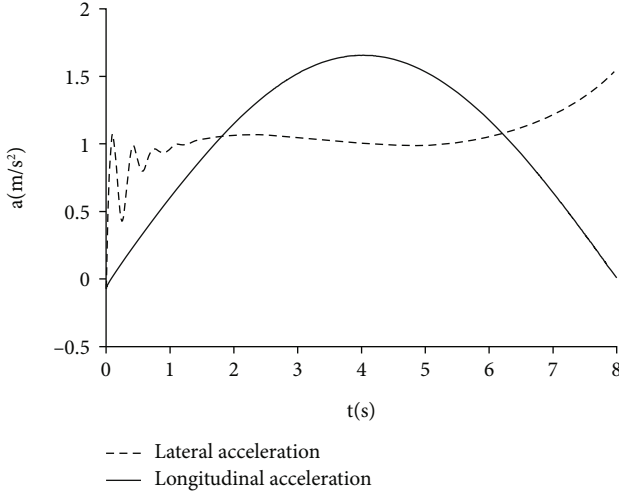


FIGURE 4: Acceleration response.

variables when designing the trajectory-tracking lateral controller. According to the desired lane-changing trajectory, the integrated active front-wheel steering trajectory-tracking controller based on feedforward and feedback is established to improve the trajectory-tracking accuracy of vehicle on the curved roads.

The lane-changing tracking is actually tracking the expected motion state. According to (16), the lateral acceleration based on the desired lane-changing trajectory can be obtained. Therefore, when the vehicle is running steadily, the relationship between the front-wheel angle and the lateral acceleration is as follows:

$$G_{a_y} = \frac{a_y(t)}{\delta_f} = \frac{v_x^2(t)}{L(1 + Kv_x^2(t))}, \quad (21)$$

where G_{a_y} is the steady-state lateral acceleration gain, K is the stability factor, and $K = (m/L^2)((l_f/k_2) - (l_r/k_1))$. Therefore, combining (16) and (21), when the vehicle tracks the lane-changing stably, the following equation is satisfied:

$$\delta_{f1} = \frac{a_y(t)}{G_{a_y}} = a_y \cdot \frac{L(1 + Kv_x^2(t))}{v_x^2(t)}. \quad (22)$$

The desired front-wheel angle can be obtained by using the feedforward control based on the expected acceleration, but the tracking accuracy cannot be guaranteed. In this section, the sliding mode variable structure control with exponential reaching law is used, and the feedback control system is designed by combining the backstepping method. The feedback correction is carried out on the basis of the feedforward control, so as to track the driving state of the vehicle. The deviation between the actual yaw angle and the expected yaw angle is taken as the tracking error

$$e_1 = \varphi - \varphi_d. \quad (23)$$

Lyapunov function is selected as

$$V_1 = \frac{1}{2} e_1^2. \quad (24)$$

The first-order derivative of (24) is obtained as

$$\dot{V}_1 = e_1 \dot{e}_1 = e_1(\dot{\varphi} - \dot{\varphi}_d). \quad (25)$$

In order to realize the tracking stability, (25) needs to satisfy $\dot{V}_1 \leq 0$, and the sliding mode function is defined as

$$s_1 = c_1 e_1 + \dot{e}_1, \quad (26)$$

where $c_1 > 0$, and the virtual control can be taken as

$$\dot{\varphi} = s_1 - c_1 e_1 + \dot{\varphi}_d. \quad (27)$$

Then, (25) can be expressed as

$$\dot{V}_1 = e_1 s_1 - c_1 e_1^2. \quad (28)$$

If $s_1 = 0$, then $\dot{V}_1 \leq 0$, and the Lyapunov stability condition is satisfied, that is, equation (22) can be stable in finite time.

According to the designed sliding mode function, the Lyapunov function is redefined as

$$V_2 = V_1 + \frac{1}{2} s_1^2. \quad (29)$$

Because of $\dot{s}_1 = c_1 \dot{e}_1 + \ddot{\varphi} - \ddot{\varphi}_d$, the first-order derivation of (29) can be obtained as

$$\begin{aligned} \dot{V}_2 = e_1 s_1 - c_1 e_1^2 + s_1 \left[c_1 \dot{e}_1 + \frac{2l_r k_2^2 + 2l_f k_1^2}{I_z v_x} \dot{\varphi} \right. \\ \left. + \frac{2l_f k_1 - 2l_r k_2}{I_z v_x} v_y + u_2 - \ddot{\varphi}_d \right], \end{aligned} \quad (30)$$

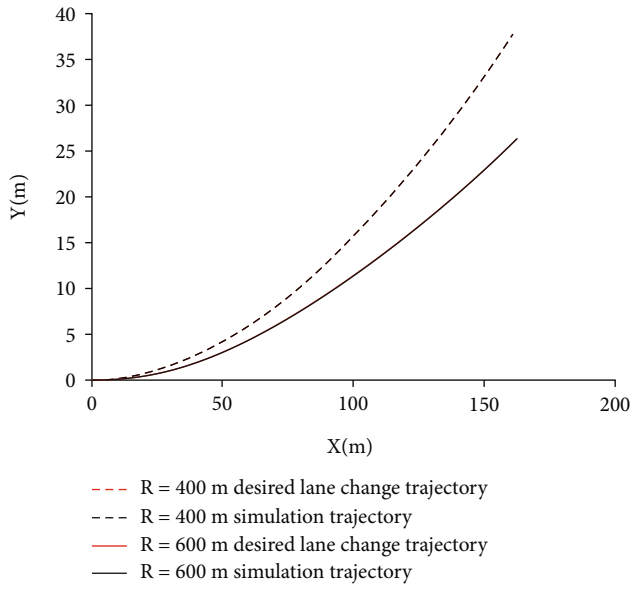
where $u_1 = F_x$, $u_2 = (\lambda F_x l_f - 2l_f k_1 / I_z) \delta_f$. In order to satisfy the requirements $\dot{V}_2 \leq 0$, the control law is designed as follows:

$$\begin{aligned} u_2 = -c_1 \dot{e}_1 - \frac{2l_r k_2^2 + 2l_f k_1^2}{I_z v_x} \dot{\varphi} - \frac{2l_f k_1 - 2l_r k_2}{I_z v_x} v_y \\ + \ddot{\varphi}_d - e_1 - \eta_1 s_1 - \lambda_1 \operatorname{sgn}(s_1). \end{aligned} \quad (31)$$

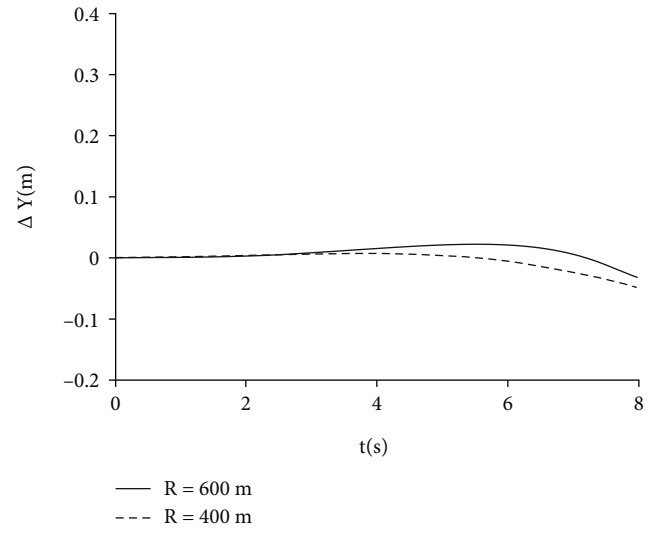
By substituting the above control law into (27), we get

$$\dot{V}_2 = -c_1 e_1^2 - \eta_1 s_1^2 - \lambda_1 |s_1|. \quad (32)$$

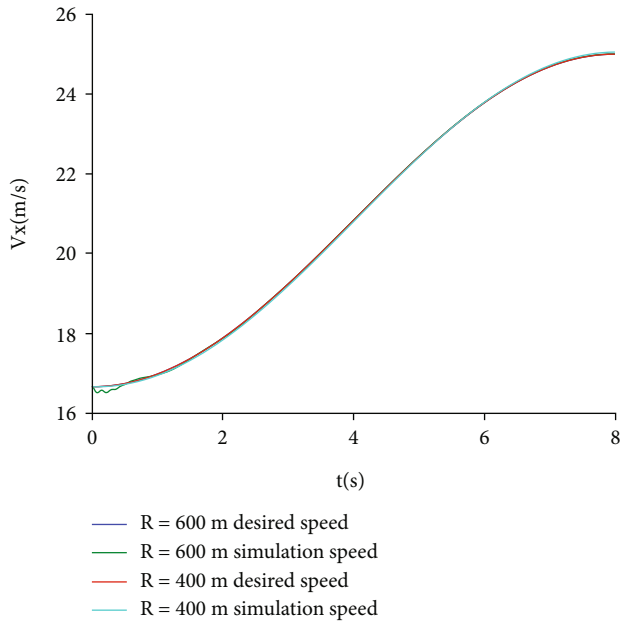
Due to $-c_1 e_1^2 - \eta_1 s_1^2 - \lambda |s_1| \leq 0$, the designed control law can ensure that the tracking error of the system converges to 0 in a limited time, and the lateral control system can track the desired yaw rate during lane-changing.



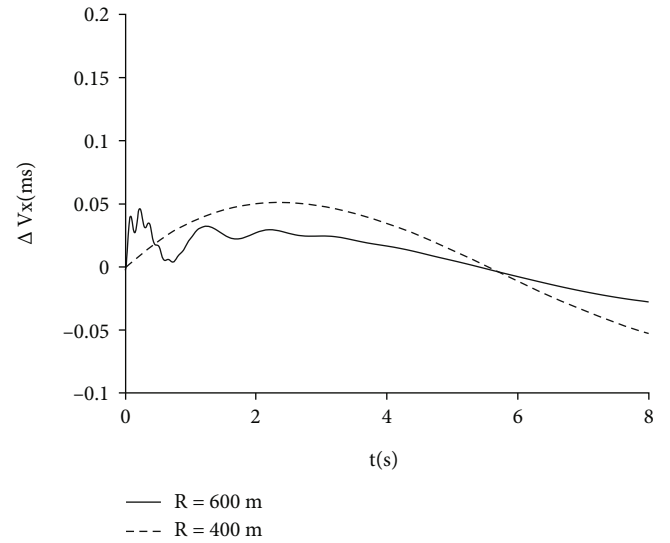
(a) Trajectory tracking



(b) Position error

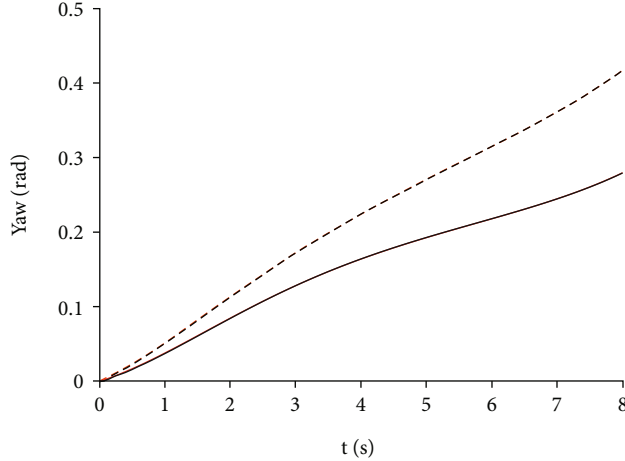


(c) Longitudinal speed



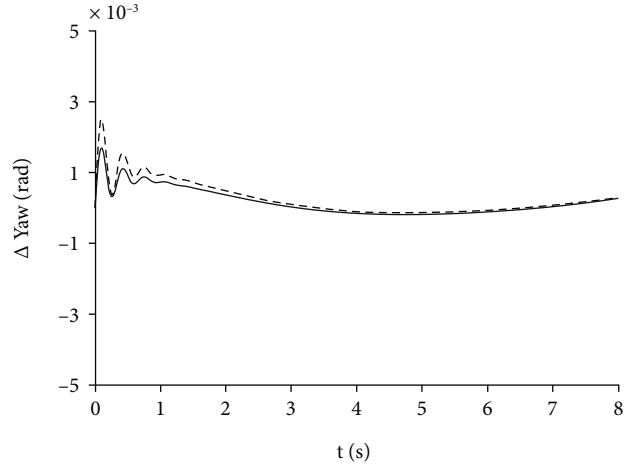
(d) Longitudinal speed error

FIGURE 5: Continued.



— R = 600 m desired yaw angle
 — R = 600 m simulation yaw angle
 - - R = 400 m desired yaw angle
 - - R = 400 m simulation yaw angle

(e) Yaw angle



— R = 600 m
 - - R = 400 m

(f) Yaw angle error

FIGURE 5: Vehicles lane-changing from outside to inside with different curvatures.

5.2. Longitudinal Control in Trajectory Tracking. The purpose of vehicle longitudinal control is to make the vehicle meet the demand of speed changing during lane-changing. The vehicle longitudinal control also adopts the backstepping sliding mode control method. The longitudinal force of the vehicle is taken as the control object, and the deviation between the actual longitudinal displacement of the vehicle and the longitudinal displacement of the desired trajectory is taken as the tracking error of the controller.

$$e_2 = X - X_c. \quad (33)$$

Similarly, the longitudinal control law in lane-changing is

$$u_1 = \frac{m}{\cos \varphi} \left[-c_2 \dot{e}_2 + v_x \dot{\varphi} \sin \varphi + \dot{v}_y \sin \varphi + v_y \cos \varphi - e_2 - \eta_2 s_2 - \lambda_2 \operatorname{sgn}(s_2) \right] - (f_R c_z - c_x) v_x^2 + m f_R g - m v_y \dot{\varphi} + 2k_1 \frac{v_y + l_f \dot{\varphi}}{v_x}. \quad (34)$$

The output of trajectory tracking controller based on backstepping sliding mode is

$$\begin{bmatrix} F_x \\ \delta_{f2} \end{bmatrix} = \begin{bmatrix} u_1 \\ \frac{I_z u_2}{\lambda l_f F_x - 2 l_f k_1} \end{bmatrix}, \quad (35)$$

where $\lambda_1 > 0$, $\eta_1 \geq 0$, $\lambda_2 > 0$, and $\eta_2 \geq 0$.



FIGURE 6: Hardware-in-the-loop test platform.

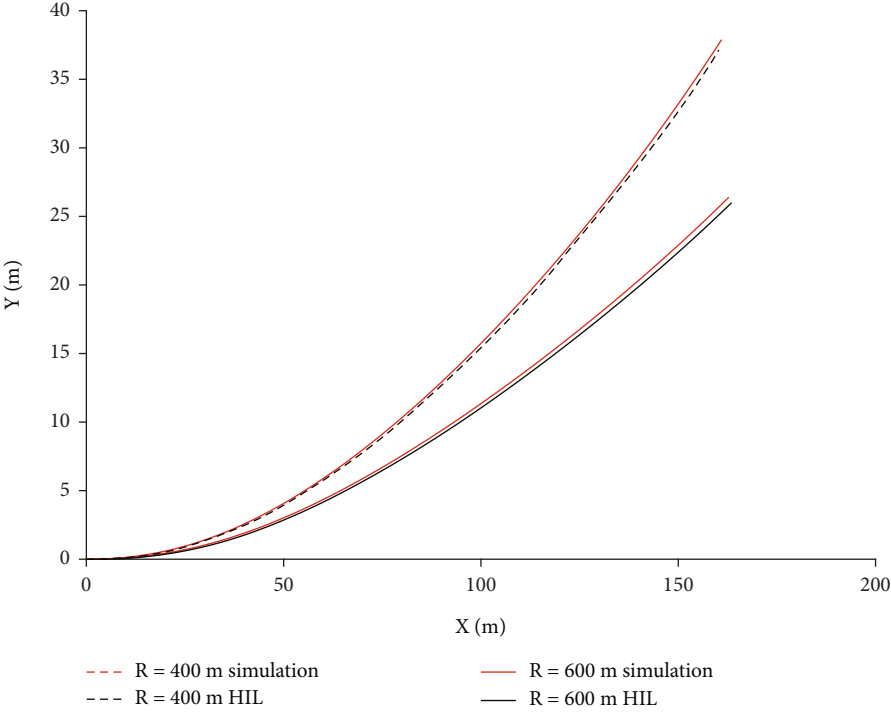
In conclusion, the output of the active lane-changing controller is

$$\begin{cases} F_x = u_1, \\ \delta_f = \delta_{f1} + \delta_{f2}. \end{cases} \quad (36)$$

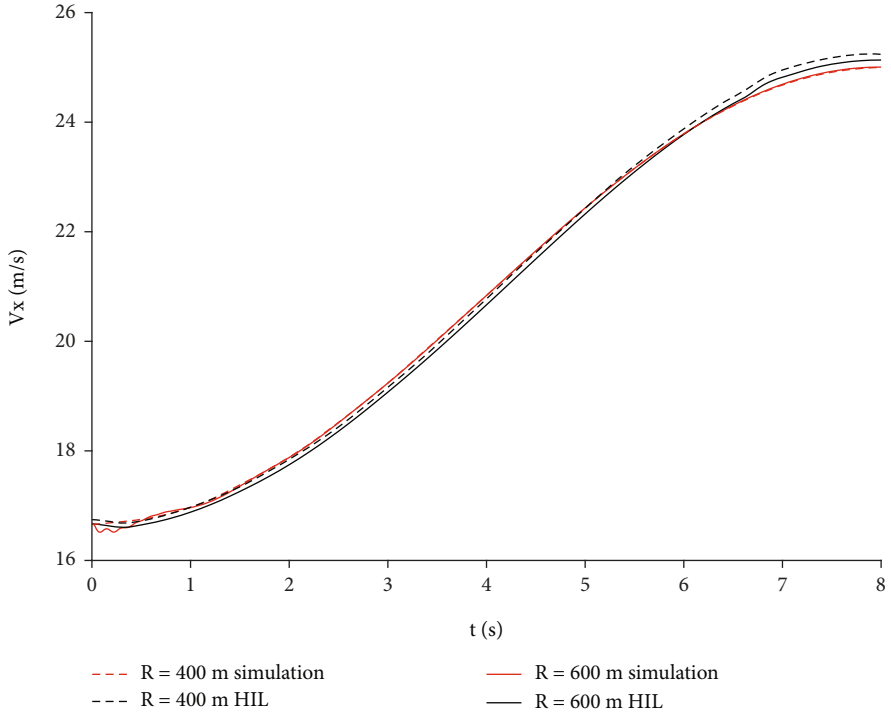
6. Simulation and Analysis

In order to verify the effectiveness of the trajectory tracking control algorithm proposed in this paper, the traditional trajectory tracking control method (preview control method) [19] is selected for comparison. The parameters required for simulation are shown in Table 1.

6.1. Simulation under the Same Lane-Changing Condition. The driving condition as the two-lane road is set with 400 meters curvature radius, and the road is under good driving condition with the adhesion coefficient $\mu = 0.8$.

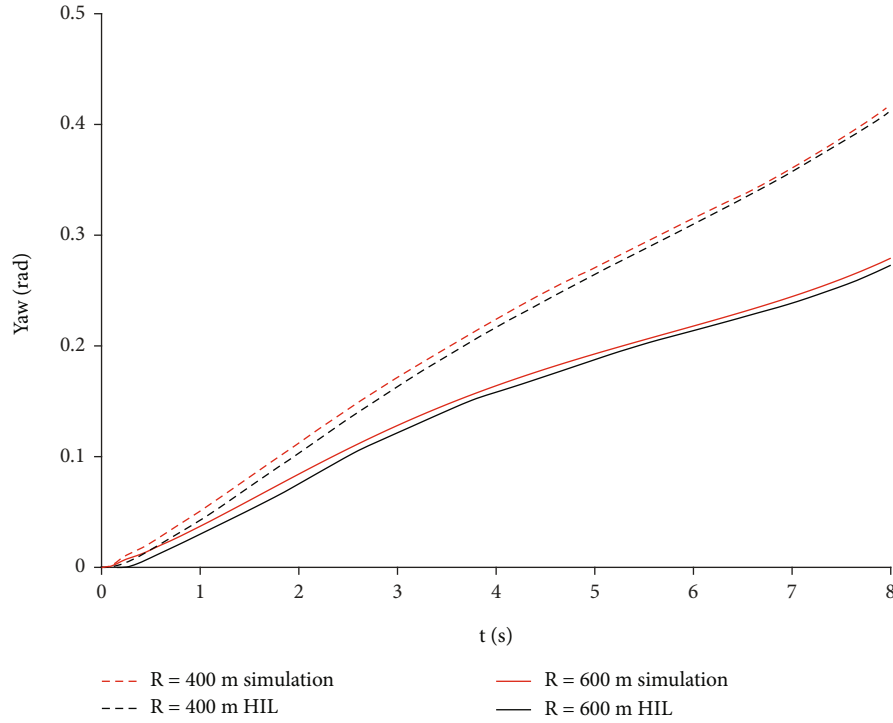


(a) Trajectory tracking



(b) Longitudinal speed

FIGURE 7: Continued.



(c) Yaw angle tracking

FIGURE 7: HIL test results.

According to the limited speed requirements of different lanes of the expressway, vehicles need to accelerate when changing lanes to meet the speed requirements of the target lane. Therefore, according to the minimum road speed requirements, the current-lane driving speed is set as 60 km/h, and the target speed is 90 km/h at the end of lane change. The center line radius of the outer lane is 400 m, and the lane change time is set as 8 s.

Figures 3(a) and 3(b) show the trajectory tracking and lateral position error, respectively. It can be seen from Figure 3(a) that the lane-changing trajectory generated by the proposed trajectory planning method can be tangent to the center line of the target lane, and the trajectory curvature changes continuously without mutation. It can be seen from Figure 3(b) that the maximum lateral position error of the trajectory tracking control strategy proposed in this paper is only -0.047 m. However, the maximum value of lateral position error based on preview follow control is 0.205 m, and the lateral error at the end of lane change is 0.175 m, which deviates from the center line of the target lane.

Figures 3(c) and 3(d) show yaw angle and yaw angle error, respectively. It is obvious that the two control methods have good control effect of yaw angle tracking. But it can be seen from Figure 3(d) that the yaw angle tracking error with the control strategy proposed in this paper is less than 0.001 rad, and the tracking effect is more stable and the tracking accuracy is higher. Through comparison, it can be seen that the designed trajectory tracking controller in this paper has better trajectory tracking effect.

As shown in Figure 4, the maximum value of lateral acceleration during lane-changing is 1.64 m/s^2 , and the maximum

value of longitudinal acceleration is 1.69 m/s^2 . Lateral motion state meets the lateral motion stability requirements of (16), and the longitudinal acceleration curve satisfies the general form of sine curve.

6.2. Simulation under Different Road Curvatures. In order to verify that the proposed trajectory planning and tracking control method can meet the needs of lane-changing under different curvatures, two kinds of curved roads with radius 400 m and 600 m are set for lane-changing simulation test under the same working condition.

It can be seen from Figures 5(a) and 5(e) that when the radius is 400 m, the maximum yaw angle required to complete lane-changing is 0.416 rad, and the maximum vehicle trajectory on y -axis is $Y_{\max} = 37.65 \text{ m}$. When the radius is 600 m, the maximum yaw angle required to complete lane-changing is 0.279 rad, and the maximum vehicle trajectory on y -axis is $Y_{\max} = 26.6 \text{ m}$. It can be found out that the larger the radius, the smoother the lane change trajectory. By comparing the errors of Figures 5(b) and 5(f), when the radius is 600 m, the maximum lateral error at the end of lane-changing is 0.032 m, which is 0.015 m less than that at the end of lane-changing when the radius is 400 m, and the yaw angle error is smaller. It can be concluded that the trajectory planning and tracking control method designed in this paper has better tracking effect on the curve with the larger radius. It can be seen from Figures 5(c) and 5(d) that after changing the curve radius, the control results of the longitudinal speed are basically the same, and the speed tracking error is smaller when the curvature is larger.

TABLE 2: Tracking state error at the end of $T = 8$ s.

	$R = 600$ m	$R = 400$ m
Y (m)	0.139	0.383
ΔV_x (m/s)	-0.08	-0.135
ΔYaw (rad)	0.005	0.006

7. Hardware-in-the-Loop Test

In order to further verify the effectiveness of the designed trajectory tracking control algorithm and the correctness of the simulation analysis, the HIL test is carried out for the designed algorithm. The simulation scene and data acquisition interface are established in the upper computer and then downloaded to the lower computer based on LabVIEW RT real-time system after compiling. The HIL test platform (shown in Figure 6) mainly includes an upper computer, steer-by-wire module, brake-by-wire module, PXI and its data acquisition card, angle torque sensor, and pressure sensor.

The HIL test condition is set to be consistent with the simulation condition. And the HIL test is carried out under the expressway curve lane-changing condition. The test results of the track tracking, yaw angle tracking, and speed control in the lane-changing process are compared and analyzed.

It can be seen from the results shown in Figure 7 that the HIL test and simulation analysis have the same driving trend. Table 2 shows the deviation between the simulation analysis results and the HIL test results when $t = 8$ s, that is, the simulation values is smaller to the HIL values. The data show that the HIL test results is basically consistent with the simulation and can perform lane-changing operation function accurately.

To sum up, comparing the results of HIL test and simulation analysis under two different curvature sections, it is found out that the lane-changing trajectory planning and tracking control method proposed in this paper performs well under the high-speed driving conditions. Due to the signal response delay of HIL test system, the tracking effect of the system lags behind that of the software simulation. Thus, the HIL test verifies the feasibility and effectiveness of the lane-changing trajectory planning and tracking control method proposed in this paper.

8. Conclusions

In this paper, a longitudinal and lateral coordinated trajectory planning method is proposed for vehicle active lane-changing on curved roads under the high-speed condition. On the basis of feedforward steering control, a longitudinal and lateral coordinated trajectory tracking feedback controller is designed by using inversion method and sliding mode theory, which realizes the yaw angle control and vehicle speed control while lane-changing.

The co-simulation model based on CarSim/Simulink hardware-in-the-loop test bench is built, which are carried out under different road curvature conditions to verify the

effectiveness of the proposed strategy and methods. The experimental results show that the lateral trajectory error is less than 0.1 m at the end of lane-changing, and the tracking control accuracy is higher than the traditional control method. The larger the curvature radius of the road is, the higher the tracking accuracy is, and the smaller the lateral trajectory error and vehicle speed control error are. It shows that the trajectory planning method proposed in this paper can meet the requirements of high-speed lane-changing under different curvature radius and can accurately and quickly complete the trajectory tracking control, ensuring that the lateral position error and longitudinal speed control error are kept in a small range.

In this paper, it is assumed that the driving environment of the target lane meets the lane-change requirements, and only the lane change trajectory planning and tracking in the ideal curve scene are discussed. In the future study, the influence of other vehicles in lane-changing will be fully considered, so as to achieve safer and more reasonable obstacle avoidance ability.

Data Availability

The underlying data supporting the results of your study can be found through connecting to the corresponding author and emailing him.

Conflicts of Interest

The authors declared that they have no conflicts of interest to this work.

Acknowledgments

This research was supported by the Open Research Fund of Anhui Engineering Technology Research Center of Automotive New Technique (QCKJ202002), Open Fund of the Key Laboratory of Advanced Perception and Intelligent Control of High-end Equipment of Ministry of Education (GDSC202013), and Key Natural Science Project of Education Department of Anhui Province (KJ2019A0901, KJ2020A0797-“Research on EPS/ESP control system integration under the design coordination control rules in the “person-vehicle-road” closed-loop system”).

References

- [1] S. Sai, O. Altintas, J. Kenney, H. Tanaka, and Y. Inoue, “Current and future ITS,” *IEICE TRANSACTIONS on Information and Systems*, vol. E96.D, no. 2, pp. 176–183, 2013.
- [2] R. Bishop, “Intelligent vehicle applications worldwide,” *IEEE Intelligent Systems and Their Applications*, vol. 15, no. 1, pp. 78–81, 2000.
- [3] Z. Yu, Y. Li, and L. Xiong, “A review of the motion planning problem of autonomous vehicle,” *Journal of Tongji University (Natural Science)*, vol. 45, no. 8, pp. 1150–1159, 2017.
- [4] K. G. Jolly, R. S. Kumar, and R. Vijayakumar, “A Bezier curve based path planning in a multi-agent robot soccer system without violating the acceleration limits,” *Robotics and Autonomous Systems*, vol. 57, no. 1, pp. 23–33, 2009.

- [5] M. Elbanhawi, M. Simic, and R. N. Jazar, "Continuous path smoothing for car-like robots using B-spline curves," *Journal of Intelligent and Robotic Systems*, vol. 80, no. S1, pp. 23–56, 2015.
- [6] H. U. Jing, J. I. Zhong-xun, P. E. Xiao-yan, and H. U. Lin, "Driving style adaptive lane-changing trajectory planning and control," *China journal of Highway and Transport*, vol. 32, no. 6, pp. 226–239, 2019.
- [7] G. Zhuo, C. Wu, and F. Zhang, *Model predictive control for feasible region of active collision avoidance*, SAE Technical Paper, 2017.
- [8] H. J. Bai, J. F. Shen, L. Y. Wei, and Z. Feng, "Accelerated lane-changing trajectory planning of automated vehicles with vehicle-to-vehicle collaboration," *Journal of Advanced Transportation*, vol. 2017, 11 pages, 2017.
- [9] D. Soudbakhsh, A. Eskandarian, and D. Chichka, "Vehicle steering maneuvers with direct trajectory optimization," in *2010 IEEE Intelligent Vehicles Symposium*, pp. 449–453, San Diego, CA, 2010.
- [10] L. Wang, X. Zhao, H. Su, and G. Tang, "Lane changing trajectory planning and tracking control for intelligent vehicle on curved road," *Springer Plus*, vol. 5, no. 1, pp. 1150–1167, 2016.
- [11] X. Y. Wang and Q. D. Wang, "Lateral switched LMIs/ H_{∞} steering control strategy of intelligent vehicle based on path error dynamics model," *China Mechanical Engineering*, vol. 26, no. 16, pp. 2237–2243, 2015.
- [12] M. Brown, J. Funke, S. Erlien, and J. C. Gerdes, "Safe driving envelopes for path tracking in autonomous vehicles," *Control Engineering Practice*, vol. 61, pp. 307–316, 2017.
- [13] Z. Q. Liu, Y. F. Wang, and X. G. Wu, "Collision avoidance by lane changing based on linear path-following control," *China Journal of Highway and Transport*, vol. 32, no. 6, pp. 86–95, 2019.
- [14] Q. D. Wang, Y. X. Li, and W. W. Chen, "A research on emergency obstacle avoidance of intelligent vehicle based on braking and steering coordinated control," *Automotive Engineering*, vol. 41, no. 4, pp. 395–403, 2019.
- [15] T. Peng, L. L. Su, Z. W. Guan, R. H. Zhang, C. F. Zong, and J. K. Li, "A safe lane-change model for vehicle emergent collision avoidance on curved section of highway," *Automotive Engineering*, vol. 41, no. 9, pp. 1013–1020, 2019.
- [16] W. Chen, R. Zhang, L. Zhao, H. Wang, and Z. Wei, "Control of chaos in vehicle lateral motion using the sliding mode variable structure control," *Proceedings of the Institution of Mechanical Engineers, Part D: Journal of Automobile Engineering*, vol. 233, no. 4, pp. 776–789, 2019.
- [17] M. X. Wei and M. Y. Yan, "Control algorithm on automotive emergency collision avoidance based on road surface identification," *Journal of Automotive Safety and Energy*, vol. 8, no. 4, pp. 359–366, 2017.
- [18] L. Guo, X. H. Huang, P. S. Ge, G. X. Zhang, and M. Yue, "Lane changing trajectory tracking control for intelligent vehicle on curved road based on backstepping," *Journal of Jilin University (Engineering and Technology Edition)*, vol. 43, no. 2, pp. 323–328, 2013.
- [19] S. S. Qiu, L. J. Qian, and J. H. Lu, "Lane change control of intelligent vehicle based on optimal preview," *China Mechanical Engineering*, vol. 30, no. 23, pp. 2778–2783, 2019.